MSUCP-40
April 1982

Neutron Shielding Calculations for Phase II Operations of the National Superconducting Cyclotron Laboratory

J. Naryanaswamy, J. Duffy, E. Kashy, Z. Koenig and R.M. Ronningen

National Superconducting Cyclotron Laboratory
Michigan State University
East Lansing, MI 48824

I. INTRODUCTION

The coupled superconducting cyclotron currently under construction at the NSCL on the Michigan State University campus will, when completed, provide experimentalists with a wide range of heavy ion beams (from ^{4}He to ^{238}U), energies (up to 200 MeV/A), and intensities (up to 10^{13} particles/sec.). Beams with these characteristics produce copious amounts of penetrating radiation, the most important being neutrons. A broad spectrum of neutron energies results from interactions with the beam-stopping material. A significant fraction of the neutrons have velocities nearly the same as the beam velocity.

The purpose of this report is to calculate neutron radiation exposure of laboratory personnel (dose rates) for the expected typical operations of the facility. In doing this, an expected operations mode is first defined: available beams, intensities, and facility usage in terms of target areas and tuning areas. Secondly, models of neutron production in heavy ion reactions are investigated and utilized to predict neutron yields. Finally, dose rates are calculated for key areas within the facility, outside the experimental vaults. Radiation external to the facility, from "skyshine", is also estimated.

The major focus of this study is to attain low, short-term, dose rates (<2.5 mRem/hr) just outside shielding walls by designing local iron shielding surrounding beam dumps and stops. This local shielding, when combined with the

concrete shielding provided in the facility construction will ensure that the integrated exposure of personnel will be well below the 5 Rem/yr (whole body dose) maximum permissible exposure of radiation workers. A set of neutron monitors will insure that such levels are not exceeded. These detectors will be interlocked with the radio frequency accelerating voltage systems of the cyclotrons. The operator must then control the beam intensity so as not to exceed the operating criteria for that beam.

Table 1 gives current guidelines for radiation exposure. All laboratory personnel are radiation workers, in view of Michigan State University guidelines[1] which we follow. Standards, rules, and procedures of the University are based upon the U.S. Nuclear Regulatory Commission code of Federal Regulations, Title 10, Parts 19 and 20, and the Michigan Department of Public Health, Division of Radiological Health Regulations, "Ionizing Radiation Rules Governing Radioactive Material and Electronic Product Radiation". NSCL has published a radiation safety manual (MSUCP-38) which restates the above standards, rules and procedures, and gives procedures specific to the facility.

II. FACILITY OPERATIONS

Figure 1 shows the facility in Phase II. The experimental area floor plan is shown in Fig. 1A, and the facility and its surrounding area are shown in Fig. 1B. The radiation shielding will consist of concrete walls (thicknesses as shown) and local iron shielding (discussed below). Local shielding will be required wherever the beam is stopped, mainly at Faraday cups at the ends of beam lines, and at beam defining slits and stops in the beam transport system. These locations are labeled in the figure and are further specified in Table 2.

Experimentalists at NSCL were interviewed to determine the species, energies, and intensities of ions they expect to use in their experiments, as well as the experimental equipment they plan to use. A projection of how much time a given beam with a given intensity will be used in each experimental area was then made, and the results are summarized in Table 3. Conservatively, the beam energies and intensities are upper limits. It should be noted that the percent-time/yr adds to 80%; we assume 20% accelerator maintenance time and that the cyclotrons' duty factors are each 100%.

Representative points outside the experimental halls were chosen to study the neutron dose rates there. These are the cyclotron console area, the visitor reception area, and an area in the east side lobby. These points are noted in Fig. 1.

We have written a computer code which models the facility operation and calculates in a semi-empirical way the neutron energy spectra at given locations within the laboratory. The experimental sites in Fig. 1 and Table 1 are given x-y coordinates with respect to the origin at the K800 cyclotron. The point at which the neutron spectrum is to be calculated is also given coordinates. Angles, measured from the 0^{o} lines defined by the beam lines of the radiation sources, are then internally computed. For each source (beam stop or dump) the neutron yield is calculated from the production cross section in a "thick target" calculation. This is done for the specific angle to the test point. The concrete thickness of shielding walls is fixed in the input. The yield is further attenuated by the R^{-2} dependence of flux from a point source. This is the well known "Moyer model" for neutron attenuation. The attenuating effect of local shielding is also included. The result is the energy spectrum of neutrons at the test point. The integrated flux and dose rate are then computed. The program can loop over all beam stops, dumps, and beams for one representative point. Specific calculations are described below.

III. MODEL FOR PREDICTING NEUTRON PRODUCTION

Our model for energetic neutron production in heavy ion collisions is based on two major mechanisms, namely the "moving thermal source" and projectile fragmentation. For the moving source, one finds, qualitatively, that cross sections for light particle production can be well described in terms of a Maxwellian distribution observed in a rest frame that moves at slightly less than half the beam velocity, once a correction has been made for the Coulomb interaction with the target nucleus. The relativistic expression for the cross section can be written[2]

$$E d^2\sigma/p^2 dp d\Omega = N'_{MS} (E-\beta p\cos\theta)\exp[-\gamma(T-\beta p\cos\theta)/T_{MS}]. \qquad (1)$$

(The variables in Eq. (1) are described below.)

A second mechanism, important for lighter projectiles, and dominant in the forward direction ($\theta \leq 40^\circ$), is projectile fragmentation. Here the source moves in the beam direction with the beam velocity. Combining the two mechanisms, the functional form for the differential cross section obtained is[3]

$$d^2\sigma/d\Omega dE = p\{(Ed^2\sigma/p^2 dp d\Omega)_{MS} +$$

$$N'_F\gamma'(E-\beta' p\cos\theta)\exp[-(p^2(\cos^2\theta(\gamma'^2-1)+1)$$

$$+ \gamma'^2\beta' E(\beta' E-2p\cos\theta))/T_F]\}.$$

Here, N_{ms} and N_F are reaction-dependent quantities that contain target-projectile geometrical factors (given below).

The primed quantities are related to the source having the beam velocity. The parameter T_F is 7.5 MeV. It is the effective "temperature" in the fragmentation process, defining the average Fermi energy of a nucleon in nuclear matter; $\beta,\gamma,\beta',\gamma'$ are familar relativistic kinematical factors, E,p are the energy and momentum of the emitted light particle, θ is the angle of emission, and T_{MS} is the moving source temperature, estimated from the data[4] in Fig. 2. T is kinetic energy.

Data for the two processes for beam energies with E/A = 20 MeV to 1 GeV were compiled and fitted to determine N'_{MS} and N'_F. Few data exist for the energies that will be available in Phase II, especially for small angles. We fitted existing data for N'_{MS} and N'_F and extrapolated the results to Phase II operations using the semi-empirical geometry and energy dependences of the cross sections. Those data[4-7] used for the moving source calculations are shown in Table 4, and those for the fragmentation part[8] in Table 5. In the cases where both mechanisms are present N'_{MS} was found for data where $\theta \geq 45^{o}$. In column 5 of each table the geometrically dependent factors of the cross sections are given; dividing N'_{MS} and N'_F by these factors should lead to constants; in the extreme cases, an order of magnitude difference is observed. We found that in the case of fragmentation the proposed[3] geometrical part, $(1-V_c/E)A_T^{2/3}A_P^{1/3}(N_p/Z_p)$, did not describe the data as well as did a simple "$r_o A_T^{1/3}$" form, where r_o = 1.11. Some typical fits to the data are shown in Figs. 3 and 4.

The model above was developed for light charged particle emission. To use it for neutrons the Coulomb barrier was

removed, and the ratio of the number of neutrons to protons in the target was included.

The neutron flux was calculated from the beam stopping in either aluminum (at beam diagnostic points) or in the water Faraday cups. To obtain neutron yields we calculated "thick target" yields. From the parameterization of the data we have

$$d^2\sigma/dEd\Omega (\equiv \sigma(E)).$$

The yield (number of neutrons per beam particle) given by

$$Y = \int_{E_F}^{E_i} \sigma(E)/S(E)\, dE ,$$

where E_i is the beam energy, E_f is some final (cut-off) energy for neutron production (in our case we took E_F to be 5 MeV/A), and S(E) are stopping cross sections for the beam. The computer code used to calculate neutron spectra included the numerical evaluation of this integral with the appropriate stopping cross sections S(E) for aluminum and water.

To determine the stopping cross sections S(E) for the different beams in aluminum and water we used the following method. The ratio of the stopping cross section of a heavy ion in a given material to that for a proton at the same velocity is[9] to a very good approximation equal to the ratio of the squares of their effective charges times the square of the charge of the heavy ion,[9]

$$(S_{HI}/S_p)_{E/A} = (Z^*_{HI}/Z^*_p)^2 Z^2_{HI} \quad .$$

Here

$$Z^*_{HI}/Z^*_p = 1-[1.034-0.1777 \exp(-0.08114\ Z_{HI})] \exp(-A),$$

where

$$A = B + 0.0378 \sin(\pi B/2),$$

and

$$B = 0.0886\ Z_{HI}^{-2/3}(E_{HI}/25M_{HI})^{1/2}.$$

E_{HI} is the beam energy in keV, and M_{HI} is the beam particle mass in amu. Thus, S(E) for heavy ions in water or aluminum is related simply to S(E) for protons in these materials. These are tabulated[10] or easily calculated from the S(E) values for protons in hydrogen and oxygen after correcting for their abundances in water.

After determining neutron yields at a desired point the dose rates were calculated. Figure 5 shows factors[11] for flux-density-to-dose-equivalent-rate conversions for neutrons with energies varying over many orders of magnitude. We are interested in neutrons with energies $10\text{-}10^3$ MeV. The following parameterization was used.

$$\text{dose rate (mRem/hr)} = \text{flux (n/cm}^2\text{/sec)} / 11.615E^{-0.235},$$

where the flux density is taken for neutrons with energy E in MeV. The total dose rate was determined by integrating over the neutron flux energy distribution.

Our model was tested by calculating the neutron energy and angular distribution data[12] for 710 MeV α-particles on water and steel. Calculated and experimental yields for neutrons at 0^{o} and 45^{o} are compared in Fig. 6 and 7. These data are reasonably well reproduced. We conclude that our semi-empirical model can reliably predict the neutron flux from the 200 MeV/A -particle beam in Phase II.

To observe the effects of shielding, calculations were made for the 200 MeV/A ^{12}C beam stopping in the water beam dump of the 120" chamber. The neutron energy spectrum and dose rate were calculated for the point marked by "⊕" in Fig. 1A. First, the concrete wall shielding alone was included, of effective thickness 307 cm. The "half-value thicknesses"[13] of neutrons in concrete are shown in Fig. 8. Figure 9 shows the calculated neutron yield. As can be seen, the shielding has removed the low energy neutrons, but the flux of high energy neutrons whose velocities are distributed about the beam velocity is significant. It is clear that local (iron) shielding is needed. Adding 150 cm of iron around the beam dump reduces the dose rate to about 1 mRem/hr. The resulting neutron spectrum is shown in Fig. 10.

To identify beams which produce large numbers of neutrons all beams were studied at a given site (0^{o} direction for the γ-ray beam line, marked "⊠" in Fig. 1A). The results are given in Table 6. Inspection of this table shows that 150 cm of iron is adequate for ^{12}C beams and those heavier. But, for α particles an additional 50 cm of iron is required, unless the beam intensity is reduced.

IV. LOCAL SHIELDING

In order to obain a maximum dose rate of 2.5 mRem/hr outside the experimental vaults, shielding local to beam dumps and tuning beam stops is required. Iron is cost-effective for attenuating neutrons. The attenuation lengths for neutrons in iron were calculated by using those for concrete and scaling them by the ratio of densities.

Calculations for forward-directed neutrons from 200 MeV/A ^{12}C ions stopping in water show that 150 cm of iron are needed to obtain desired dose-rates. In the transverse directions 75 cm is sufficient. An initial design of the local shield is sketched in Fig. 11. The shielding may be moved from one experimental line to another. Current plans include at least one shield per vault.

In our calculations we did not assume a specific design other than that all calculations for angles between 0^{o} and 26^{o} were performed with thicknesses of 150 cm, and for angles between 26^{o} and 90^{o}, 75 cm was used. Even though the effective thicknesses are larger than 75 cm for angles in between 0^{o} and 90^{o} this was not included.

V. YEARLY INTEGRATED DOSE

Using the information contained in Tables 2 and 3 calculations were done using all beams in all experimental areas, to model the yearly operation. The neutron flux and dose rate were computed for the three test locations. The yearly integrated dose was calculated assuming a 40-hr-week and a 52-week-year. These results are shown in Table 8. It is clear that both the dose rate and yearly integrated dose are well below the maximum permissible values shown in Table 1.

We note that Table 3 shows that experimental area 6 (S-800 spectrograph) will be heavily used and would contribute significantly to the East-side Lobby point. Its beam dump is located approximately 20 ft. below the ground level (See Fig. 1). When calculating the integrated dose in Table 8 for the East-side Lobby the shielding effect of the earth and concrete was considered. For the other two points the beam dump was considered to be at the normal beam line height. This assumption negligibly affects the control console and reception area doses because these areas are in relatively backward angles; the dose of the East-side Lobby would be only 30% higher because it is in the transverse direction. Thus, we feel that the integrated doses in Table 8 are conservative projections within our model's framework.

VI. ACCIDENT SCENARIO

We consider the type of accident which can occur when within the same vault, the local shielding is at one location and the beam stops at another (due to switching magnet power supply failure, for example). This situation was simulated by having the shielding around the 60" chamber (experimental area 4) but the beam stopping in the 120" chamber Faraday cup (without shielding). The dose rate computed for a point just outside the wall, in the 0° direction, is 0.34 mRem/sec and in the direction 45° above the roof (with 2 roof beams) the dose rate is 4.76 mRem/sec. This level exceeds the set points of the neutron monitors, and the interlock system automatically shuts off the cyclotron radio frequency accelerating voltage system within a time of 1 sec.

VII. SKYSHINE

We now estimate the neutron flux at points external and distant (>100 m) from NSCL. This flux is due to direct transmission and atmosphere-scattered neutrons, whose source is taken to be a beam stopping in an iron-shielded water Faraday cup. Neutron flux in the atmospheric medium is known as skyshine. Extensive numerical treatments (e.g. Ref. 14) within shielding design studies specific to other facilities have been made to study and reduce the radiation danger because of skyshine. Here we wish to obtain an estimate of the problem, thus to see if more detailed studies are warranted.

We consider a severe operating case, viz. the radiation from the 200 MeV/A ^{12}C beam with an intensity of 5.2×10^{11} particles/sec in the 60" scattering chamber area. In Fig. 12 some linear dimensions are given and are used in neutron flux calculations outlined below. The shielding against skyshine is from concrete roof beams. We assume that a thickness of 1.37 m will suffice, this being three layers of the standard 18 inch roof beam. A thickness of 75 cm of iron, surrounding the Faraday cup, was assumed even though there can be 150 cm in the very forward direction (based on our study above). Although the path length through the concrete varies with angle (and was considered) the iron thickness was always kept at 75 cm, so our calculated flux will be somewhat overestimated.

The calculations were done as above, with these iron and concrete thicknesses, to find the flux at points on the upper roof surface. Angles as forward as $\theta = 25^{\circ}$ were used, because the vertical shielding walls (combined with the iron shields) are designed to reduce the radiation in the more forward directions. Angles back to about 135° were used, the flux being very small in more backward directions. The intensity pattern on the roof surface is clearly anisotropic because of the directional nature of the reaction cross section as well as the distortion due to differing effective concrete thicknesses for different angles. This pattern is shown in Fig. 13. The values of the flux are valid strictly only for points on the roof directly above the beam line because we assumed "azimuthal symmetry"; that is, for example, the neutron flux is the same along Line A in Fig. 12, ignoring the roof effects. We assume also that the flux values at points along such "Line A's" are equal (in Fig. 12, $\sigma_1 = \sigma_2 = \sigma_3$). This is done to simplify the numerical calculation of the skyshine flux, and again it means that this calculated flux will be somewhat overestimated.

An adequate description of the skyshine flux at a point R due to a point source empirically is given by[11]

$$\psi(R) = (aQ/4\pi R^2)(1-\exp(-R/\mu))\exp(-R/\lambda).$$

Here Q is the source strength (neutrons/sec), and a, μ, and λ are empirically determined constants. This expression is valid for R > 50 m. The behavior of large values of R is dominated by $e^{-R/\lambda}$, so λ is the attenuation length of neutrons in air.

For the case of 200 MeV/A ^{12}C the neutrons have a mean energy (at the upper roof surface) of 150 MeV or so. Thus λ = 100 m is appropriate. For 80 MeV and 10 MeV neutrons, μ is 47 and 56 m respectively.[11] So for our purposes we use μ = 40 m. The uncertainty in the calculated flux because of uncertainties in λ and μ is estimated to be smaller than 20%. The value of a = 2.8 was used.[11]

We must consider the source to be extended in our case. Fig. 14 shows the geometry of the problem. We must integrate

$$\psi(R) = (x_o a/4\pi R^2) \int_{-y_{0/2}}^{y_{0/2}} (\sigma(y)/r^2)(1-\exp(-r/\mu))\exp(-r/\lambda)dxdy,$$

where σ is the neutron flux at point (x,y) on the roof, and

$$r = r(x,y) = R[1-2\cos\gamma(y/R)+(y/R)^2]^{1/2} = Rp$$

Using the above assumption that the flux is the same for all x values in the rectangle x_o dy. We integrate numerically

$$\psi(R) = (x_o a/4\pi R^2) \int_{-y_{0/2}}^{y_{0/2}} (\sigma(y)/\beta^2)(1-\exp(-\beta R/\mu)) \times \exp(-\beta R/\lambda)dy.$$

We used $x_o = y_o = 16.2$ m, a square whose linear dimensions are defined by the 25^o limit.

Our results, for $\gamma = 25^o$, are shown in Fig. 15 and are given in Table 9. Other angles were investigated but the flux varies very little at given distances. The skyshine flux appears to be very small under the above assumptions. Certainly one of the first experiments will be to measure it once the accelerators are operating.

VIII. CONCLUSIONS

By using iron shielding located close to beam dumps and stops in addition to the concrete shielding walls the exposure of personnel to penetrating neutron radiation is reasonably minimized. It appears that the integrated yearly dose of the typical employee of the facility will be of the same order of magnitude as that received from naturally ocurring background activity(*). It should be realized that because of uncertainties in our model the dose ratio estimates may be in error by as much as a factor of 2 or more. Certainly, when the facility is first operational our calculations will be tested by measurements of neutron flux. Many methods for measuring the neutron spectrum are available.[15] One is especially promising because its sensitivity is well-matched to neutron energies from NSCL. It uses the $^{12}C(n,2n)^{11}C$ reaction, whose cross section is constant and large (~20 mb) from its threshold at 20 MeV to ~4 x 10^4 MeV. Plastic or liquid scintillators can be utilized as detectors. This laboratory has had experience in neutron detection ever since its commissioning. If measured fluxes are larger than our calculations give, any required modification of the local shielding design can be carried out.

*For reference purposes the radiation exposure of a typical person in the U.S. from natural and manmade sources is 186 mRem/yr. Of this, 80 mRem/yr is from naturally occurring sources.[16]

ACKNOWLEDGEMENTS

We wish to thank Prof. G.F. Bertsch, D.K. Scott, and G.D. Westfall for their assistance in the formulation of the neutron production model as well as suggesting data to test it.

References

1. Radiation Safety Manual, Office of Radiation, Chemical and Biological Safety, Michigan State University (1980).
2. T.C. Awes, G. Poggi, S. Saini, C.K. Gelbke, R. Legrain, and G.D. Westfall, Phys. Lett. 103B, 417 (1981).
3. G.F. Bertsch and D.K. Scott, private communication.
4. L. Anderson, Ph.D. thesis (unpublished); Lawrence Berkeley Laboratory report LBL-6767 (1977).
5. S. Nagamiya, M.-C. Lemaire, E. Moeller, S. Schnetzer, G. Shapiro, H. Steiner, and A. Tanihata, Phys. Rev. C24, 971 (1981).
6. T.C. Awes, S. Saini, G. Poggi, C.K. Gelbke, D. Cha, R. Legrain, and G.D. Westfall, MSUCL-362 (1981).
7. B. Jakobsson, L. Carlen, P. Kristiansson, J. Krumlinde, A. Oskarsson, H.-A. Gustafsson, T. Johansson, H. Ryde, G. Tibell, J.P. Bondorf, G. Fai, A.O.T. Karvinen, O.B. Nielson, M. Buenerd, J. Cole, D. Lebrun, J.M. Loiseaux, P. Martin, R. Ost, P. de Saintignon, C. Guet, E. Monnand, J. Mougey, H. Nifenecker, P. Perrin, J. Pinston, C. Ristori, F. Schussler, Phys. Lett. 102B, 121 (1981).
8. J.R. Wu, C.C. Chang, H.D. Holmgren, and R.W. Koontz, Phys. Rev. C20, 1284 (1979).
9. Handbook of Stopping Cross-sections for Energetic Ions in All Elements, J.F. Ziegler, (Pergamon Press, New York) 1980.

10. Tables of Range and Stopping Power of Chemical Elements for Charged Particles of Energy 0.05 to 500 MeV, Claude Finley Williamson, Jean-Paul Boujot, and Jean Piccard, Centre d' Etudes Nucléaires de Saclay, Report CEA-R3042, 1966.

11. Accelerator Health Physics, H. Wade Patterson and Ralph H. Thomas (Academic Press, New York) 1973.

12. R.A. Cecil, B.D. Anderson, A.R. Baldwin, R. Madey, A. Galonsky, P. Miller, L. Young, and F.M. Waterman, Phys. Rev. C21, 2471 (1980).

13. Nuclear Reaction Analysis, J.B. Marion and F.C. Young, (North-Holland Publishing Company, Amsterdam), 1968.

14. R.G. Alsmiller, Jr., J. Barish, and R.L. Childs, Particle Accelerators 11, 131 (1981).

15. "Health Physics Practices at Research Accelerators", Ralph H. Thomas, Lawrence Berkeley Laboratory Report LBL-4655, 1976.

16. Arthur C. Upton, Sci. Am. 246, 41(1982).

TABLE 1. MAXIMUM PERMISSIBLE EXPOSURE TO EXTERNAL RADIATION IN MILLIREM FOR RADIATION WORKERS

Part of Body	Weekly	Quarterly	Yearly
Whole Body, Head and Trunk, Active Blood Forming Organs, Lens of Eyes, or Gonads	100	1,250	5,000
Hands and Forearms, Feet and Ankles	1,500	18,750	
Skin of Whole Body	600	7,500	

TABLE 2. EXPERIMENTAL AREA DESCRIPTION (ORIGIN AT THE CENTER OF K-800 MeV CYCLOTRON)

Experimental Area	Description	Location Coordinates X(CM)	Y(CM)	Theta:Beam Direction
1	Precision Chamber	.37490D 04	.10973D 04	.51500D 02
2	Enge Spectrograph	.48158D 04	.10973D 04	.22000D 02
3	Gamma Ray	.54855D 04	.10057D 04	.80000D 01
4	60 In. Chamber	.65826D 04	.14476D 04	.38000D 02
5	120 In. Chamber	.74969D 04	.94490D 03	.75000D 01
6	S-800 Spectrograph	.84125D 04	.24380D 03	-.40000D 01
7	RPMS	.74066D 04	.83800D 02	-.20000D 01
8	RPMS	.58826D 04	-.30500D 02	-.20000D 01
9	RPMS	.46634D 04	.00000D 00	-.20000D 01
10	RPMS	.41758D 04	.00000D 00	.20000D 01
11	TUNING	.20117D 04	.15240D 03	.00000D 00

TABLE 3: PROJECTED BEAM AND EXPERIMENTAL AREA USEAGE IN PHASE II AT NSCL

BEAM	E/A (MeV)	PARTICLE CURRENT	PERCENT TIME/YR.	FRACTIONAL TIME IN EXPERIMENTAL AREAS										
				1	2	3	4	5	6	7	8	9	10	11
4He	200	1.56×10^{12}	5.0	.0	.0	.0	.40	.00	.40	.00	.00	.0	.0	.20
12C	200	5.20×10^{11}	5.0	.0	.0	.0	.12	.20	.24	.06	.06	.06	.06	.20
16O	200	3.90×10^{11}	10.0	.0	.0	.0	.12	.20	.24	.06	.06	.06	.06	.20
20Ne	200	3.12×10^{11}	15.0	.0	.0	.0	.12	.20	.24	.06	.06	.06	.06	.20
40Ar	200	1.73×10^{11}	15.0	.0	.0	.0	.12	.20	.24	.06	.06	.06	.06	.20
76Ge	125	1.04×10^{11}	7.5	.0	.0	.0	.0	.0	.0	.20	.20	.20	.20	.20
86Kr	105	1.01×10^{11}	7.5	.0	.0	.0	.0	.0	.0	.20	.20	.20	.20	.20
208Pb	20	2.60×10^{10}	7.5	.0	.0	.80	.0	.0	.0	.0	.0	.0	.0	.20
238U	20	2.50×10^{9}	7.5	.0	.0	.80	.0	.0	.0	.0	.0	.0	.0	.20

TABLE 4: DATA FOR MOVING SOURCE AND MOVING SOURCE + FRAGMENTATION REACTIONS.

Reaction	References	E/A (MeV)	Process[a)]	N_{MS}	$N'_{MS}/(1-V_c/E)(A_T^{1/3}+A_p^{1/3})^5$ (E/A) (x 10^{-4})
C(C,p)	4	1050	MS+F	918	4.35
KCl(Ar,p)	5	800	MS+F	5521	4.93
KCl(p,p')	5	800	MS+F	493	4.05
Au(O,p)	2	19	MS	99	1.67
Zr(O,p)	6	19	MS	258	9.34
C(C,p)	7	86	MS	39	2.27
Al(C,p)	7	86	MS	59	1.69
Cu(C,p)	7	86	MS	105	1.28
Ag(C,p)	7	86	MS	308	2.13
Au(C,p)	7	86	MS	291	1.02

[a]MS = moving source, F = fragmentation

TABLE 5. DATA FOR FRAGMENTATION REACTIONS USED FOR DETERMINING N_F'

Reaction	Reference	E/A (MeV)	N_F'	$N_F'/1.11A_T^{1/3}$
Al(α,p)	8	40	54.5	16.3
Ni(α,p)	8	40	73.6	17.1
Zr(α,p)	8	40	82.1	16.5
^{209}Bi(α,p)	8	40	101.1	15.4

TABLE 6. CALCULATIONS OF DOSE RATES IN FORWARD DIRECTION OUTSIDE OF SHIELD WALL FOR BEAMS STOPPING AT γ-RAY SITE.

Beam	Energy/nucleon (MeV/A)	Particle Current (10^{12} sec^{-1})	Local Shielding Thickness (cm of iron)	Dose-Rate (mRem/hr)
^{4}He	200	1.56	0	1.6×10^{4}
			150	49
			200	0.4
^{12}C	200	0.52	0	5.9×10^{3}
			150	1.8
^{16}O	200	0.39	0	4.0×10^{3}
			150	1.2
^{20}Ne	200	0.31	0	2.9×10^{3}
			150	0.9
^{40}Ar	200	0.17	0	1.4×10^{3}
			150	0.4
^{76}Ge	125	0.10	0	59
			150	1.2×10^{-2}
^{86}Kr	105	0.10	0	18
			150	2.8×10^{-3}
^{208}Pb	20	0.026	0	4.4×10^{-6}
			150	0
^{238}U	20	0.0025	0	4.2×10^{-7}
			150	0

TABLE 7. TYPICAL DOSE RATES WHEN RUNNING A 200 MeV/A ^{12}C BEAM WITH 5.2×10^{11} PARTICLES/SEC INTENSITY.

Area[a]	Beam Dump Location	Effective Concrete thickness (cm)	Local Shield Thickness(cm)	Dose Rate (mRem/hr)
Cyclotron Control Console	tuning area(b)	869.1	75	$<10^{-3}$
Reception Area	precision chamber(c)	154.6	150	1.2×10^{-1}
East-side Lobby	60" Chamber(c)	290.7	150	1.9×10^{-2}

a) The (x,y) coordinates, in units of cm, for the console, reception, and lobby areas are (2490.8, 2980.0), (4284.5, 4216.5), and (8422.5, 4267.2) respectively.

b) Stopping material is aluminum.

c) Stopping material is water.

TABLE 8. YEARLY INTEGRATED DOSE FROM PROJECTED "TYPICAL" FACILITY OPERATIONS.

Area	Neutron Flux (n/cm^2 /sec)	Dose Rate (mRem/hr)	Yearly Integrated Dose (Rem/yr)
Cyclotron Control Console	9.3×10^{-4}	2.5×10^{-4}	5.3×10^{-4}
Reception area	1.6×10^{-1}	9.1×10^{-3}	1.9×10^{-2}
East-side Lobby	1.2×10^{-2}	3.6×10^{-3}	7.5×10^{-3}

TABLE 9. DOSE RATES FROM SKYSHINE AT DISTANCES R FROM NSCL WHEN RUNNING A 200 MeV/A ^{12}C BEAM WITH 5.2×10^{11} PARTICLES/SEC INTENSITY.

Distance R (m)	Neutron Flux Intensity at R ($\gamma = 25^{o}$) (Neutrons/cm^2/sec)	Equivalent Dose Rate (mRem/hr)
100	1.9×10^{-1}	2.4×10^{-2}
200	4.5×10^{-2}	9.0×10^{-3}
300	1.8×10^{-2}	3.6×10^{-3}
400	9.0×10^{-3}	1.8×10^{-3}
500	5.2×10^{-3}	1.0×10^{-3}
600	3.3×10^{-3}	6.6×10^{-4}
700	2.2×10^{-3}	4.4×10^{-4}
800	1.5×10^{-3}	3.0×10^{-4}
900	1.1×10^{-3}	2.2×10^{-4}
1000	7.8×10^{-4}	1.6×10^{-4}

Figure Captions

FIG. 1A. Experimental area plan for NSCL in Phase II (coupled superconducting cyclotrons). Those areas studied, listed in Table 2, are marked in the figure, as well as the location of several representative points at which the integrated yearly dose was calculated.

1B. The NSCL building and its surrounding area. Note the area control fence which limits public access to the South and East sides of the facility.

FIG. 2. Data on temperatures of moving sources, obtained from measuring emitted protons (p), deuterons (d), and tritons (t) (Ref. 4). The moving source temperatures used for neutron emission were taken from the proton data.

FIG. 3. Calculation of proton energy spectrum, for $\theta = 90^{\circ}$, for the reaction $^{27}Al(^{12}C,px)$ at 86 MeV/A. The data are taken from Ref. 7. The constant N_{MS} (= N'_{MS} x geometrical and reaction factors) is an average from our survey.

FIG. 4. Calculation of neutron energy spectrum, for $\theta = 20^{\circ}$, for the reaction $^{27}Al(^{4}He,px)$ at 20 MeV/A. The data (projectile fragmentation) are taken from Ref. 8. N_F = 16.33, from our survey.

FIG. 5. Conversion factors for neutron flux density to equivalent dose-rate (Ref. 11). The parameterization of the data for $10\text{-}10^3$ MeV neutrons is given in the text.

FIG. 6. Comparison of calculation (solid line) to data (x) on neutron yields from 720 MeV α-particles on water (Ref. 12). The neutron emission angle was $\theta = 0^{\circ}$.

FIG. 7. Comparison of calculation (solid line) and data (x) on neutron yields from 720 MeV α-particles on water (Ref. 12). The neutron emission angle was $\theta = 45^{\circ}$.

FIG. 8. Half-value thicknesses for neutrons in concrete (Ref. 13).

FIG. 9. Neutron energy spectrum at a distance of 9.25 m from a water Faraday cup in which 800 MeV α-particles are stopped. There is no local shielding, and 3 m of concrete from the shielding walls.

FIG. 10. Neutron energy spectrum at a distance of 9.24 m from a water Faraday cup in which 800 MeV α-particles are stopped. There is 150 cm of iron as local shielding as well as 3 m of concrete from the shielding walls.

FIG. 11. Preliminary design of a local iron shield.

FIG. 12. a) Side view showing some dimensions in the area of the 60" scattering chamber. These dimensions were used for skyshine calculations. b) A view along the beam direction, corresponding to line A in a). σ_1, σ_2, and σ_3 represent neutron flux values, the flux being a function of position on the roof.

FIG. 13. Neutron flux angular distribution at the roof surface. The angle θ is defined in Fig. 12.

FIG. 14. Geometry used for the "extended source" calculation of the neutron flux at a distance R from the roof.

FIG. 15. Skyshine neutron flux as a function of distance from the roof beam. Here, $\gamma = 25^{\circ}$ (R and γ are shown in Fig. 14).

MSUX-82-050

RECEPTION

EASTSIDE LOBBY POINT

Y
N
X

CYCLOTRON CONSOLE

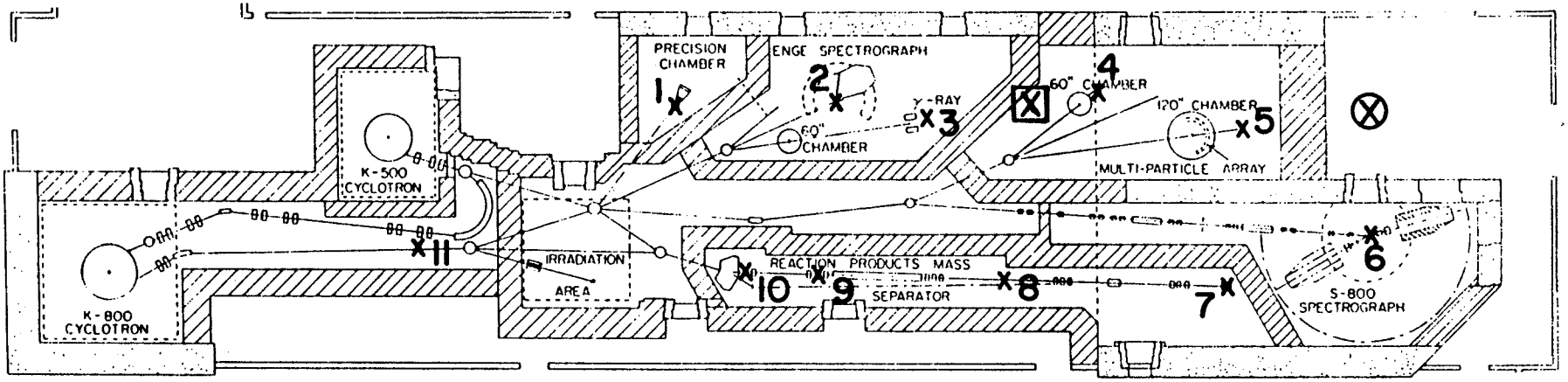

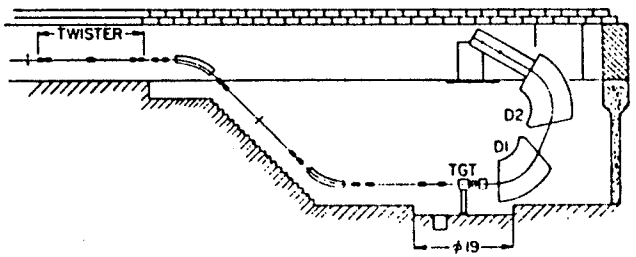

NSCL - PHASE II
EXPERIMENTAL AREAS

SCALE 1" = 1175.2 cm

MSUX-82-051

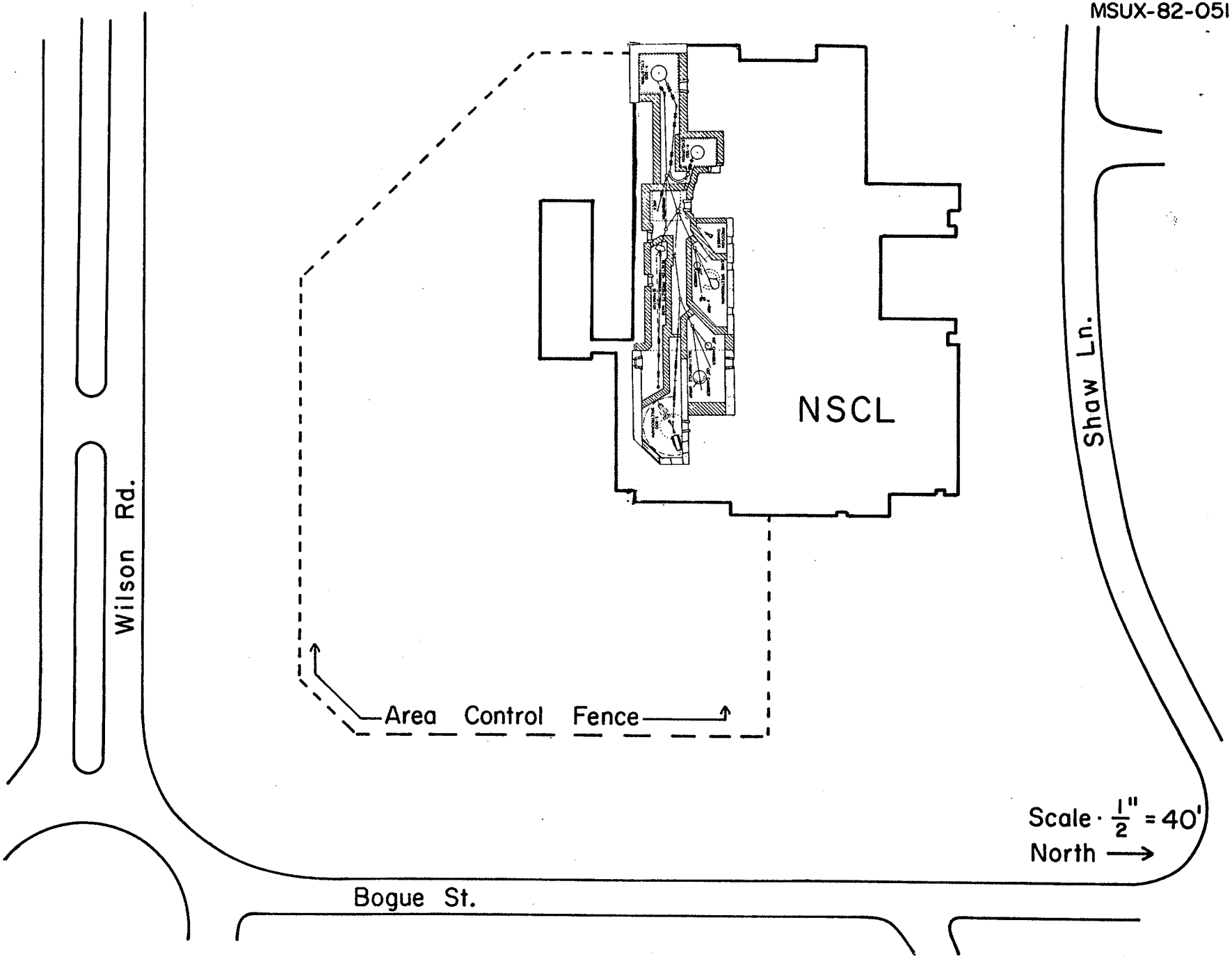
NSCL
Wilson Rd.
Shaw Ln.
Area Control Fence
Bogue St.
Scale · 1/2" = 40'
North

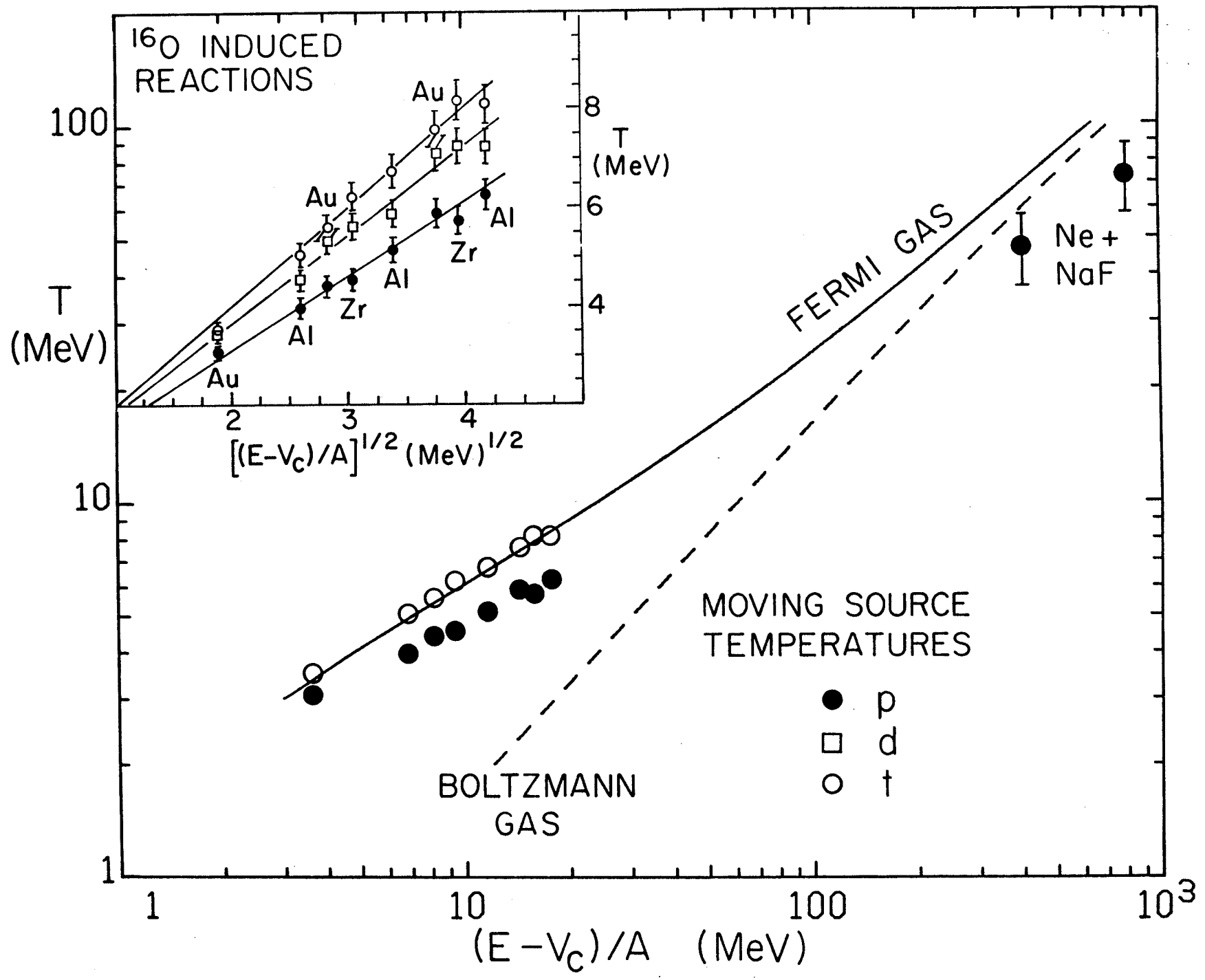
^{16}O INDUCED REACTIONS
Au
Au
Al
Zr
Al
Zr
Au
Al
T (MeV)
8
6
4
2
3
4
$[(E-V_c)/A]^{1/2}$ (MeV)$^{1/2}$
100
10
1
T (MeV)
FERMI GAS
Ne + NaF
MOVING SOURCE TEMPERATURES
p
d
t
BOLTZMANN GAS
1
10
100
10^3
$(E-V_c)/A$ (MeV)

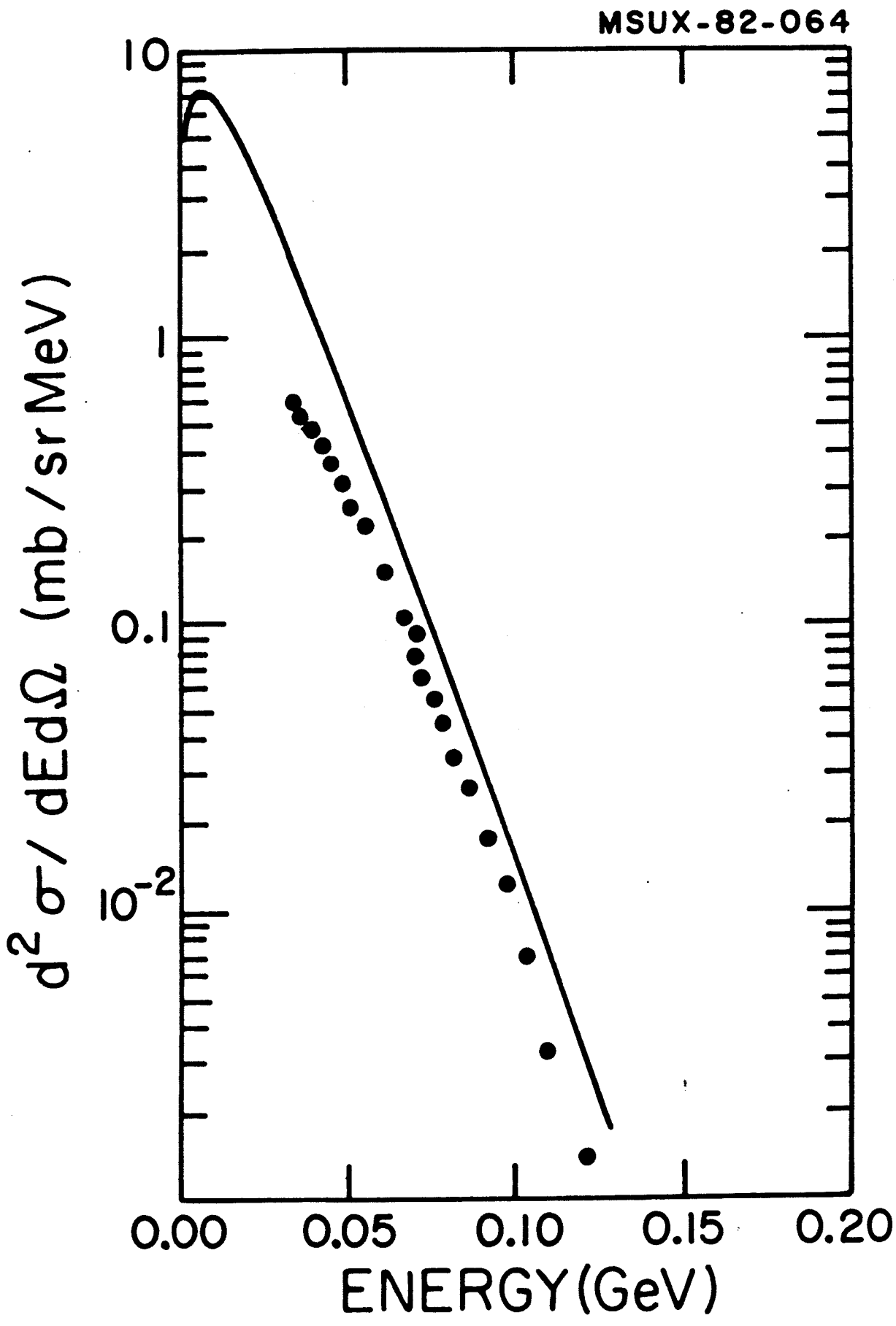
MSUX-82-064
10
1
0.1
10^{-2}
$d^2\sigma / dEd\Omega$ (mb / sr MeV)
0.00
0.05
0.10
0.15
0.20
ENERGY (GeV)

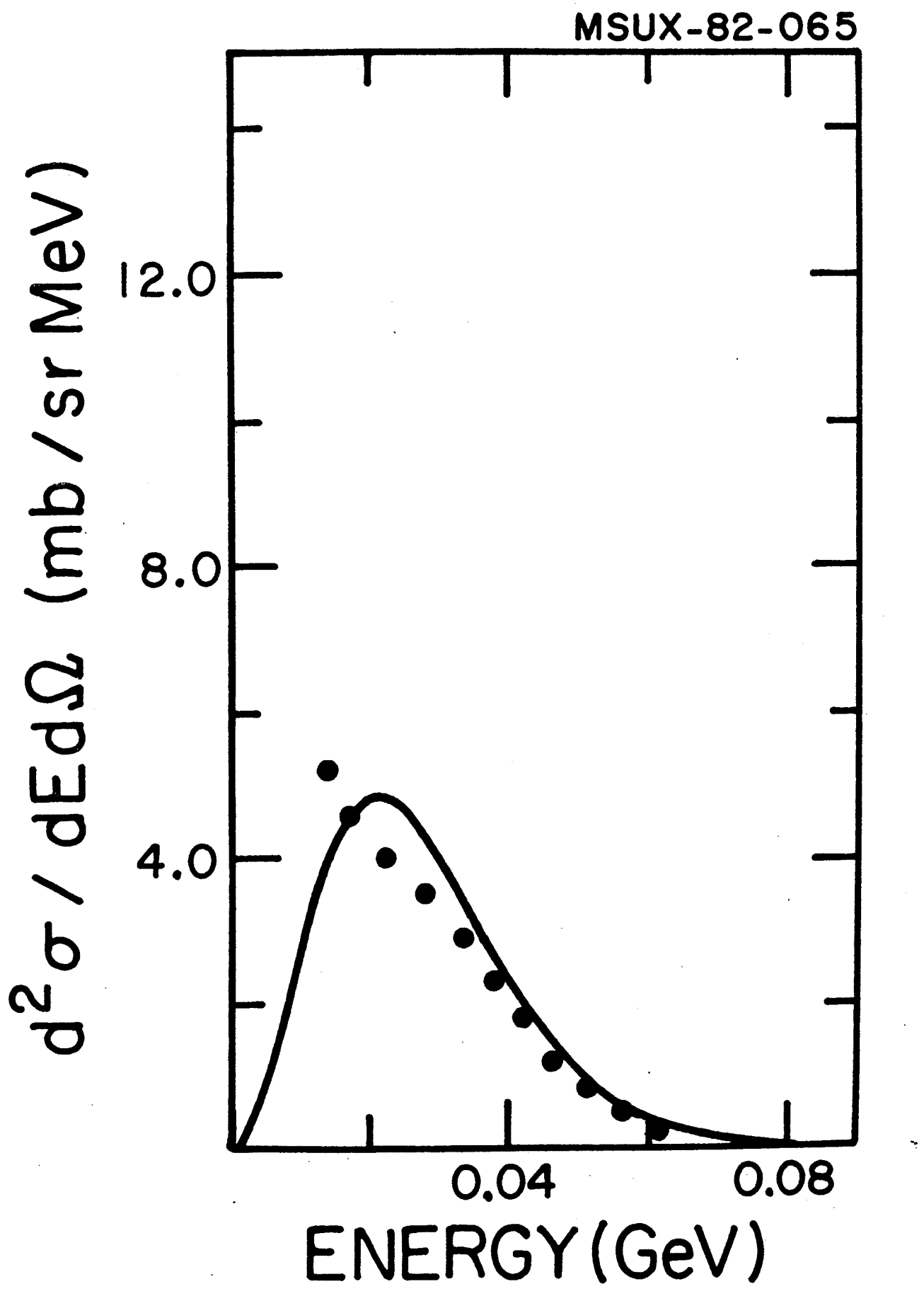
MSUX-82-065
$d^2\sigma / dEd\Omega$ (mb / sr MeV)
12.0
8.0
4.0
0.04
0.08
ENERGY (GeV)

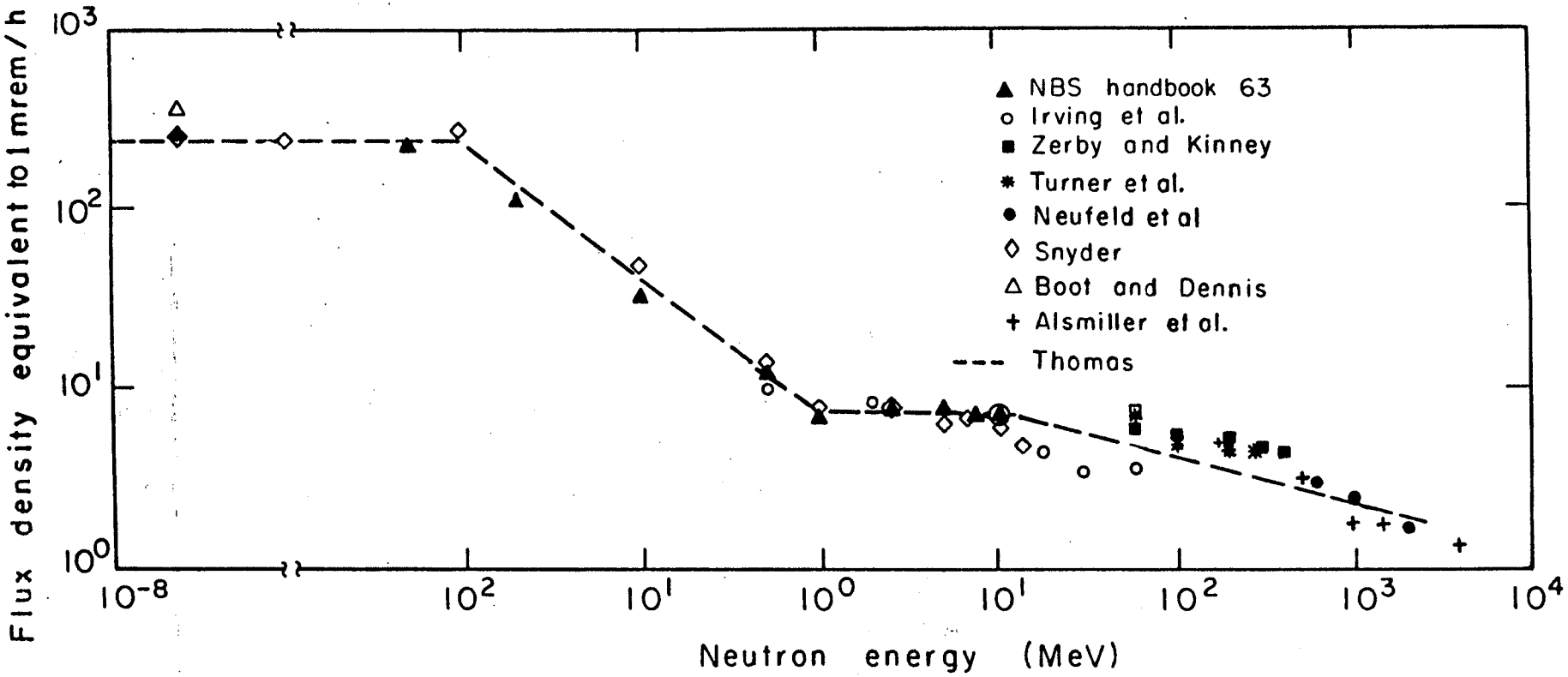
Flux density equivalent to 1 mrem/h
10^3
10^2
10^1
10^0
10^{-8}
10^2
10^1
10^0
10^1
10^2
10^3
10^4
Neutron energy (MeV)
▲ NBS handbook 63
o Irving et al.
■ Zerby and Kinney
* Turner et al.
● Neufeld et al
◇ Snyder
△ Boot and Dennis
+ Alsmiller et al.
--- Thomas

XBL703-2499

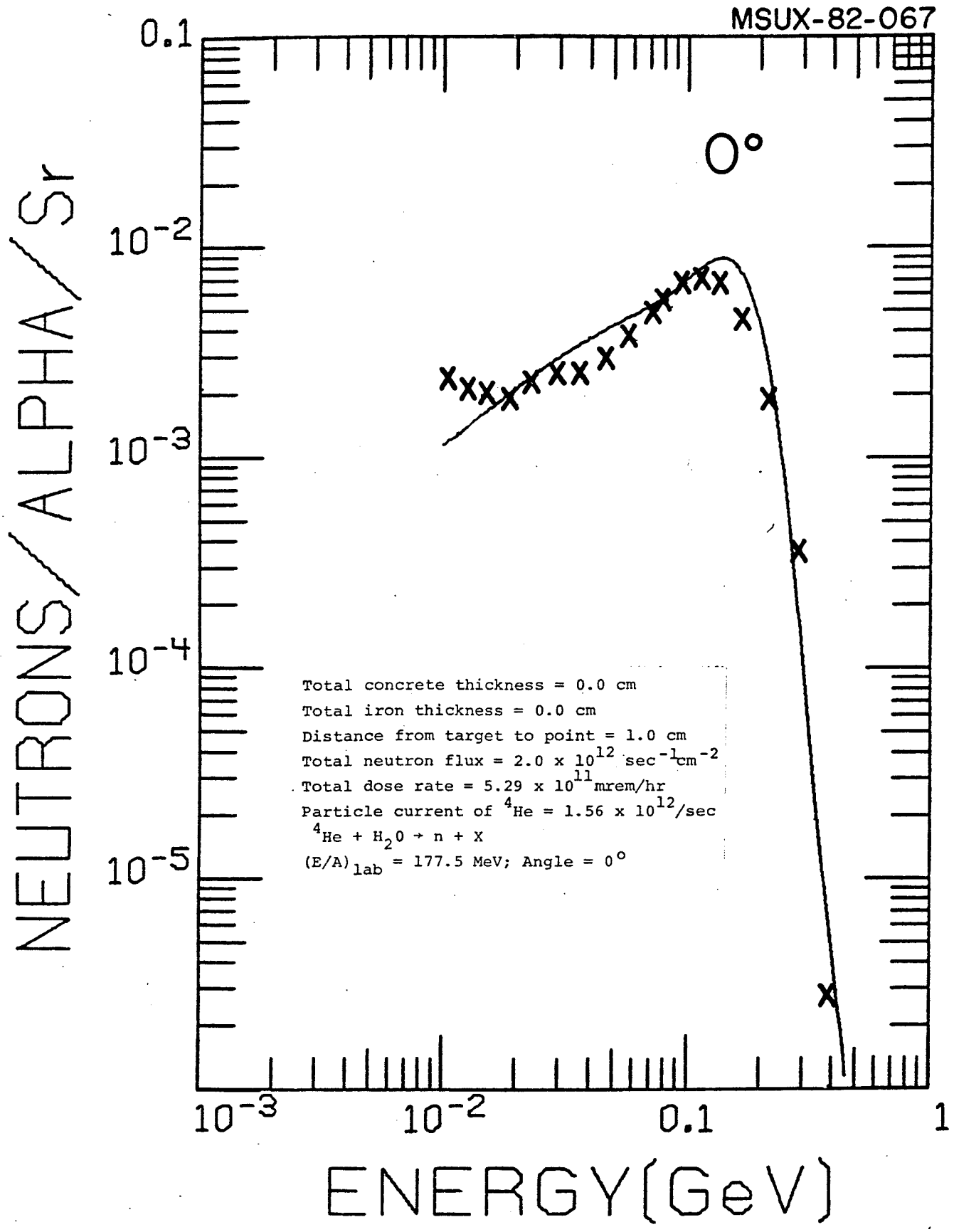
MSUX-82-067
0°
NEUTRONS/ALPHA/Sr
ENERGY(GeV)
0.1
10^{-2}
10^{-3}
10^{-4}
10^{-5}
10^{-3}
10^{-2}
0.1
1
Total concrete thickness = 0.0 cm
Total iron thickness = 0.0 cm
Distance from target to point = 1.0 cm
Total neutron flux = 2.0 x 10^{12} $sec^{-1}cm^{-2}$
Total dose rate = 5.29 x 10^{11} mrem/hr
Particle current of ^4He = 1.56 x 10^{12}/sec
$^4He + H_2O \rightarrow n + X$
$(E/A)_{lab}$ = 177.5 MeV; Angle = 0°

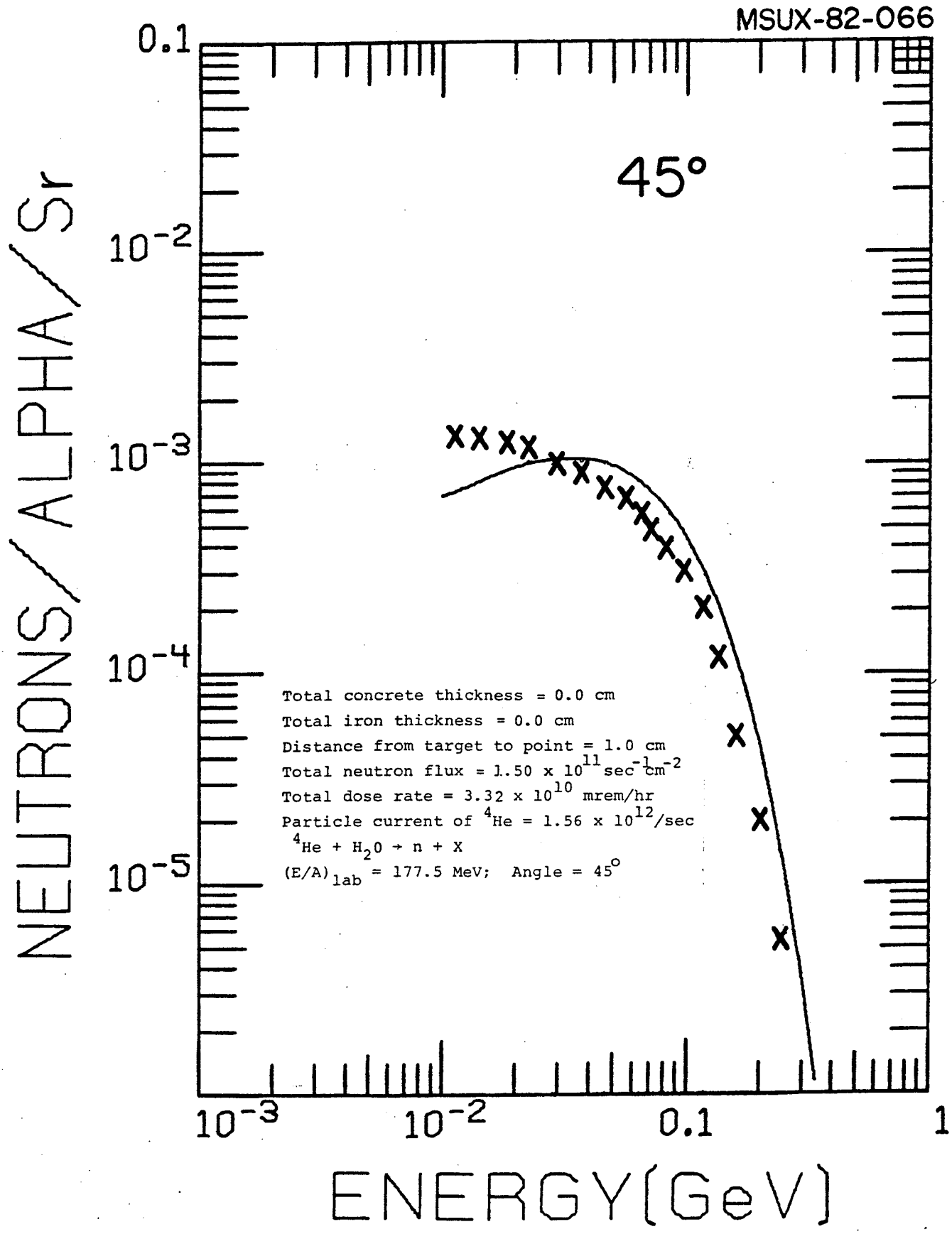
MSUX-82-066
45°
NEUTRONS/ALPHA/Sr
ENERGY(GeV)
0.1
10^{-2}
10^{-3}
10^{-4}
10^{-5}
10^{-3}
10^{-2}
0.1
1
Total concrete thickness = 0.0 cm
Total iron thickness = 0.0 cm
Distance from target to point = 1.0 cm
Total neutron flux = 1.50×10^{11} $sec^{-1}cm^{-2}$
Total dose rate = 3.32×10^{10} mrem/hr
Particle current of ^4He = 1.56×10^{12}/sec
$^4He + H_2O \rightarrow n + X$
$(E/A)_{lab}$ = 177.5 MeV; Angle = 45°

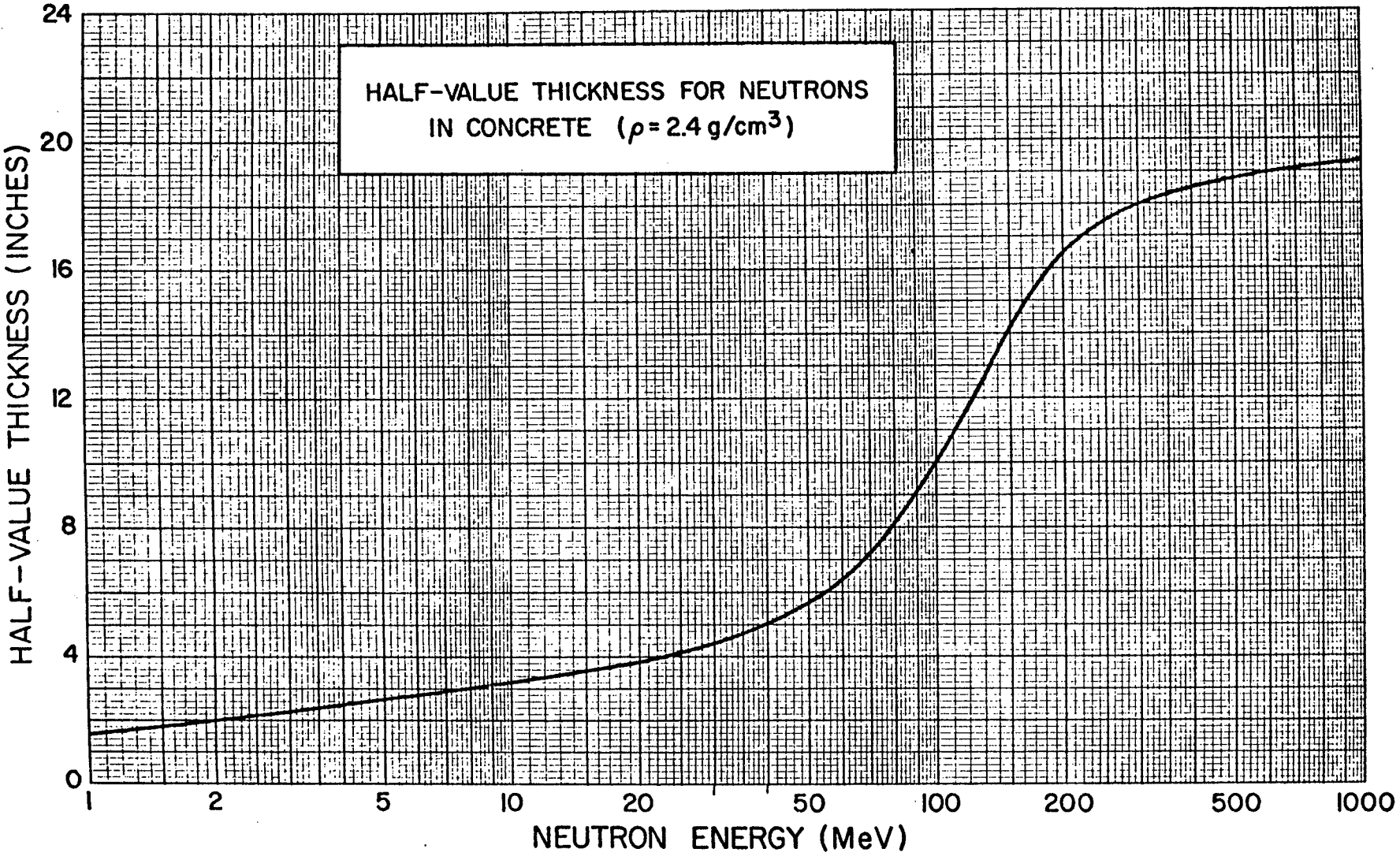
HALF-VALUE THICKNESS FOR NEUTRONS
IN CONCRETE ($\rho = 2.4\ g/cm^3$)
HALF-VALUE THICKNESS (INCHES)
0
4
8
12
16
20
24
1
2
5
10
20
50
100
200
500
1000
NEUTRON ENERGY (MeV)

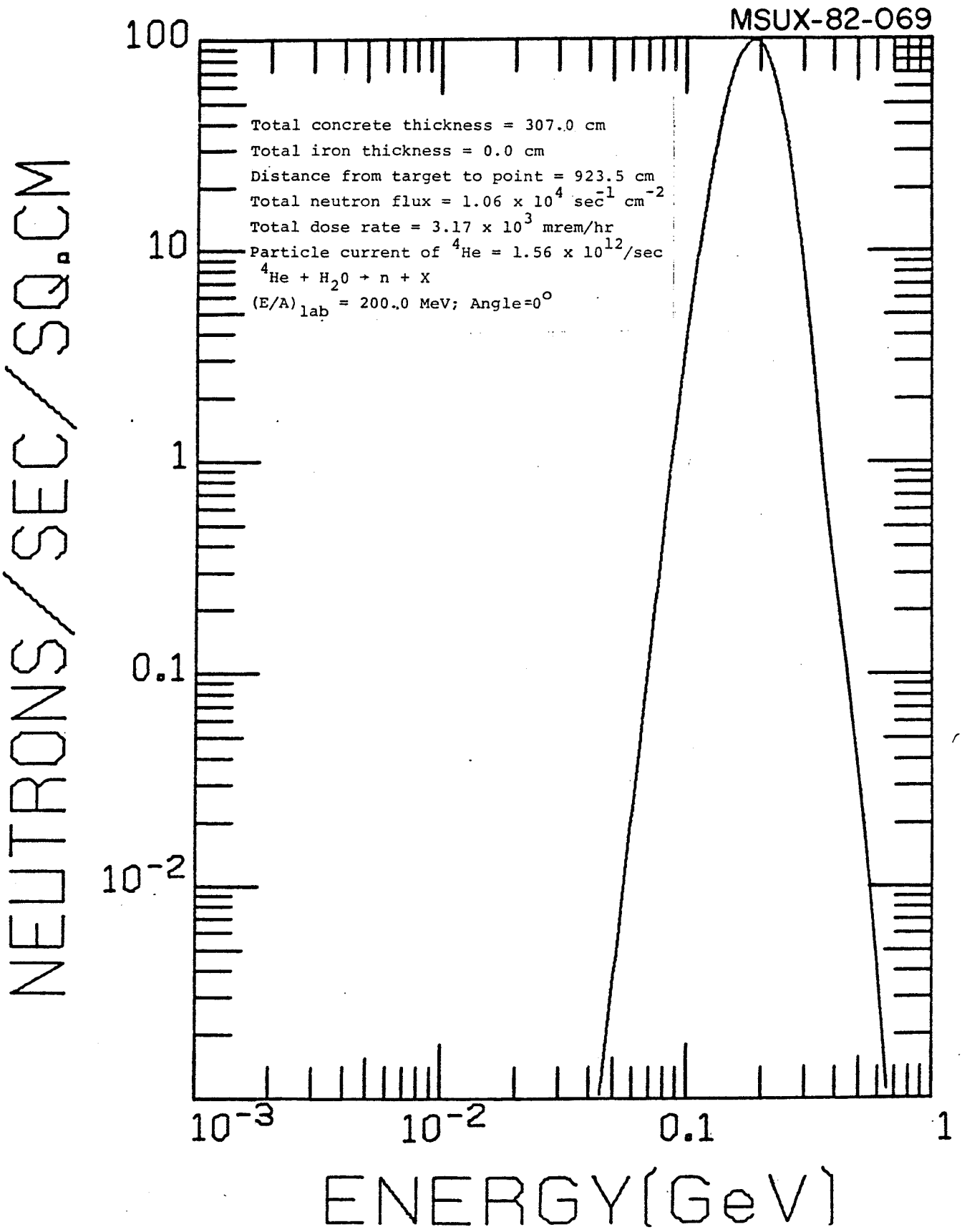
MSUX-82-069
Total concrete thickness = 307.0 cm
Total iron thickness = 0.0 cm
Distance from target to point = 923.5 cm
Total neutron flux = 1.06 x 10^4 sec^-1 cm^-2
Total dose rate = 3.17 x 10^3 mrem/hr
Particle current of 4He = 1.56 x 10^12/sec
4He + H20 → n + X
(E/A)lab = 200.0 MeV; Angle=0°
NEUTRONS/SEC/SQ.CM
100
10
1
0.1
10^-2
10^-3
10^-2
0.1
1
ENERGY(GeV)

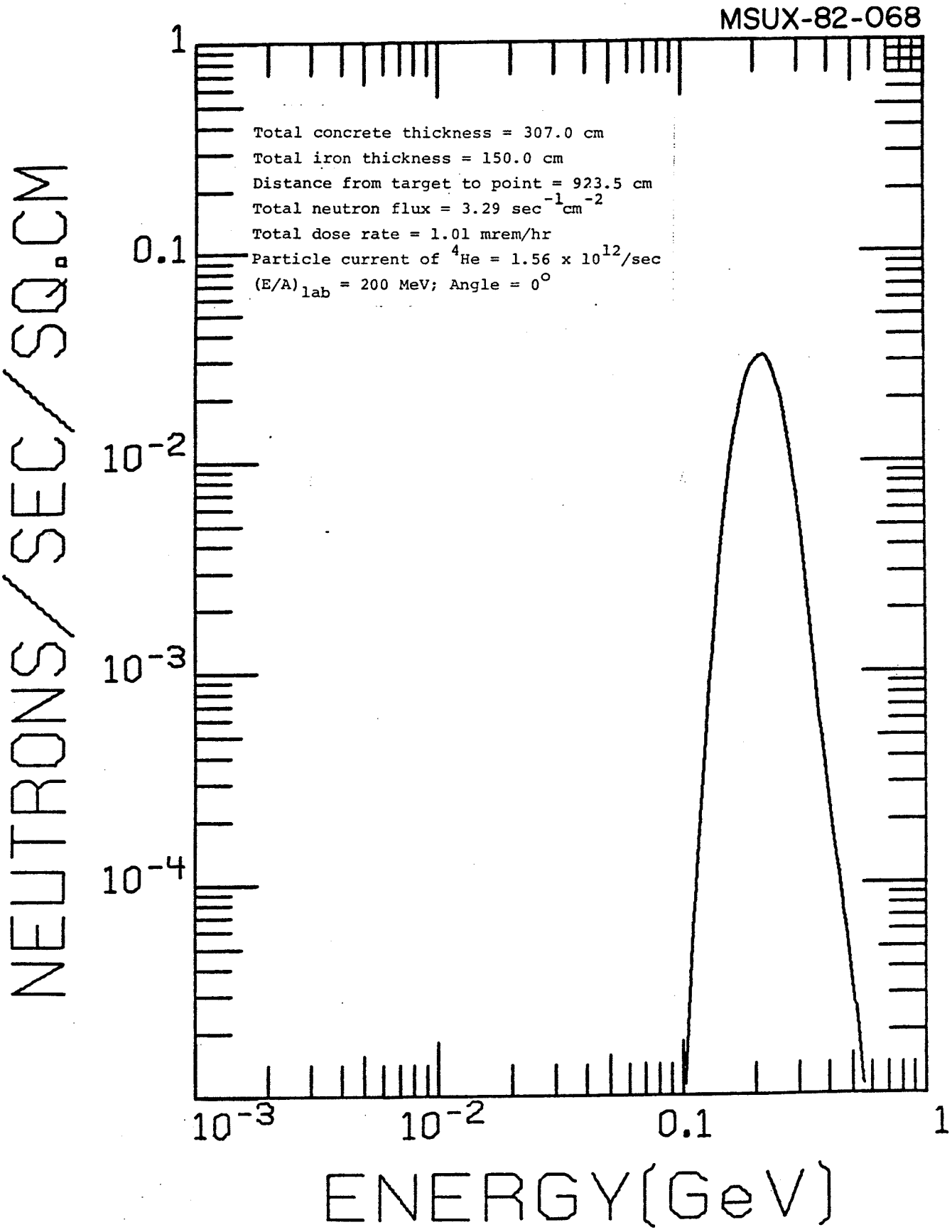
MSUX-82-068
Total concrete thickness = 307.0 cm
Total iron thickness = 150.0 cm
Distance from target to point = 923.5 cm
Total neutron flux = 3.29 sec^{-1}cm^{-2}
Total dose rate = 1.01 mrem/hr
Particle current of ^{4}He = 1.56 x 10^{12}/sec
$(E/A)_{lab}$ = 200 MeV; Angle = 0°
NEUTRONS/SEC/SQ.CM
1
0.1
10^{-2}
10^{-3}
10^{-4}
10^{-3}
10^{-2}
0.1
1
ENERGY(GeV)

MSUX-82-041

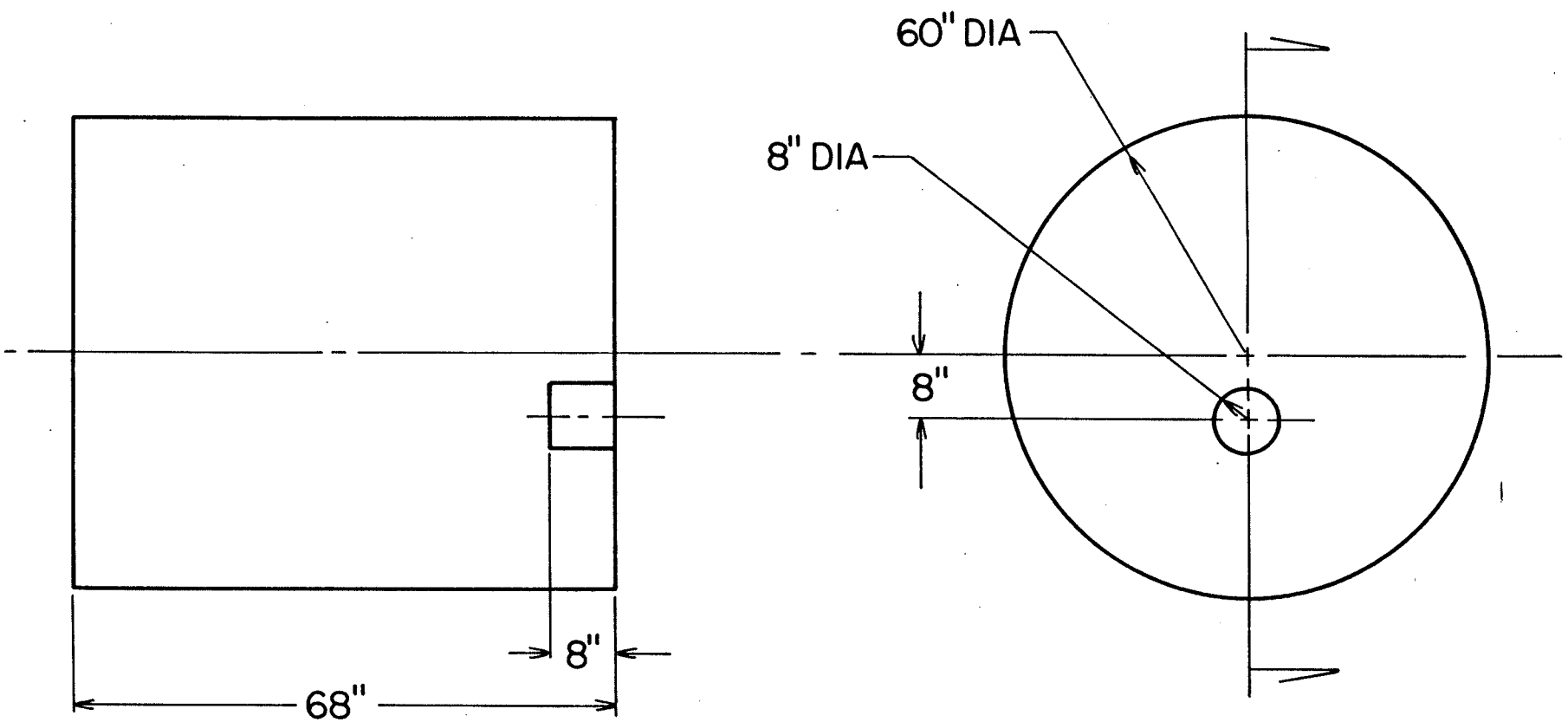

LOCAL IRON SHIELDING
FOR FARADAY CUP (PHASE II)

MATERIAL: IRON
ESTIMATED SIZE: 60" DIA × 68"
ESTIMATED WEIGHT: 27 TONS

MSUX-82-038

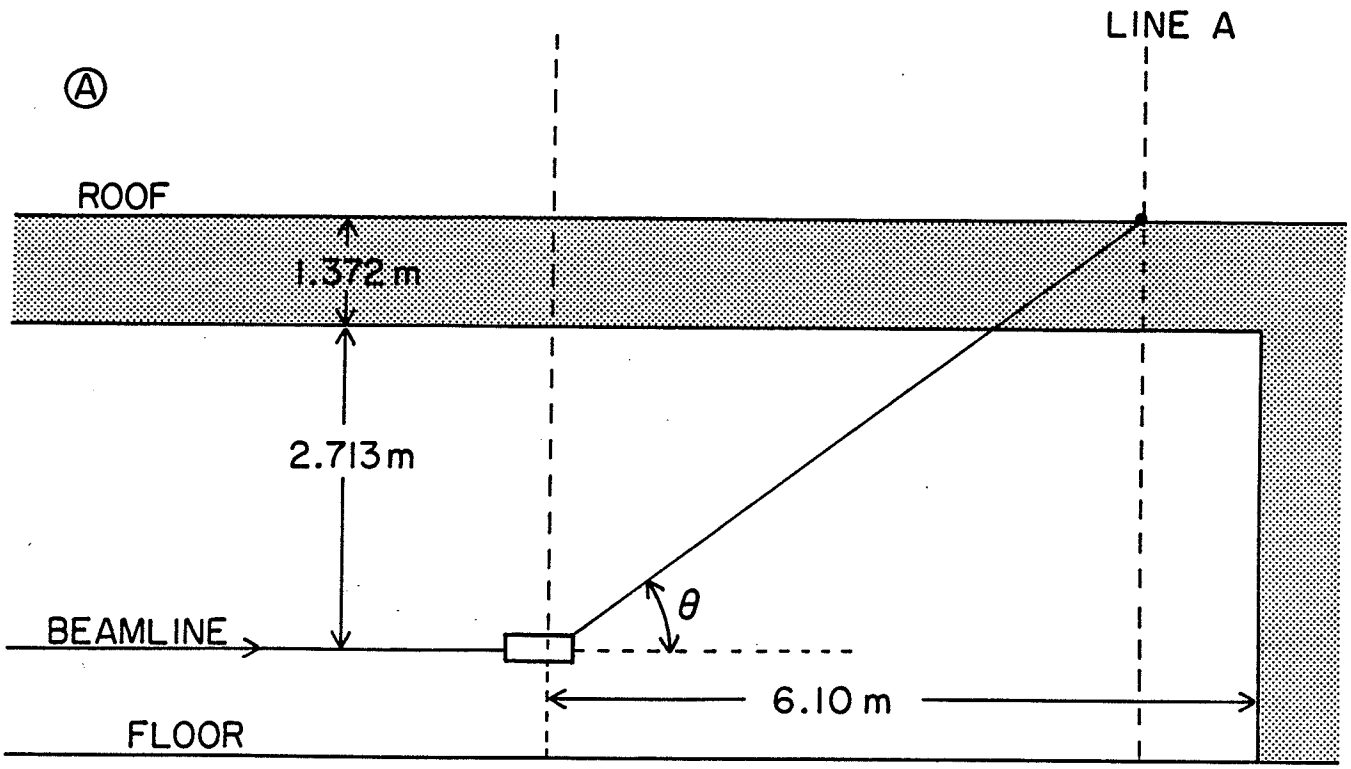
LINE A
Ⓐ
ROOF
1.372 m
2.713 m
θ
BEAMLINE
6.10 m
FLOOR

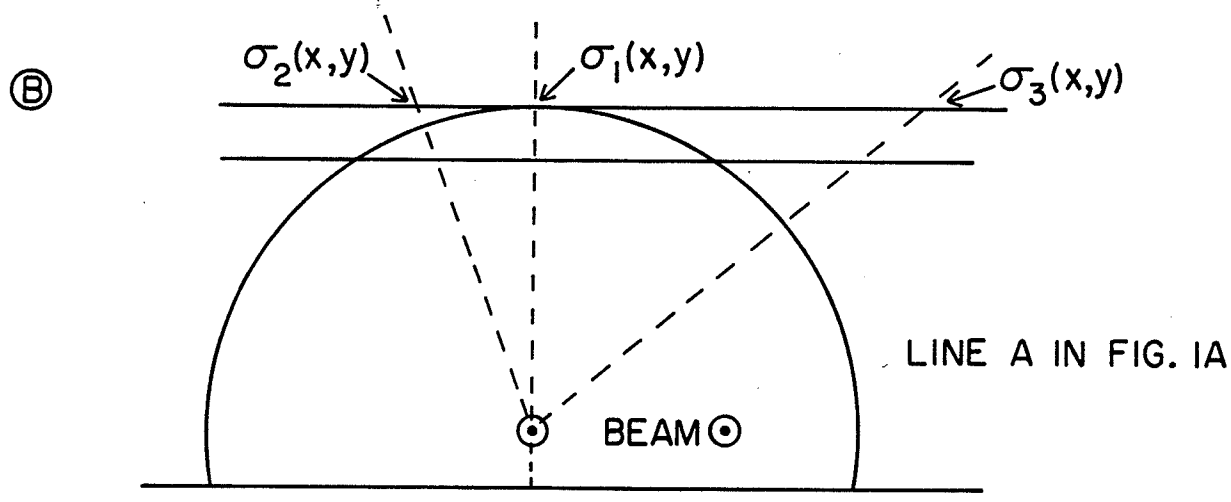
Ⓑ
$\sigma_2(x,y)$
$\sigma_1(x,y)$
$\sigma_3(x,y)$
BEAM ⊙
LINE A IN FIG. IA

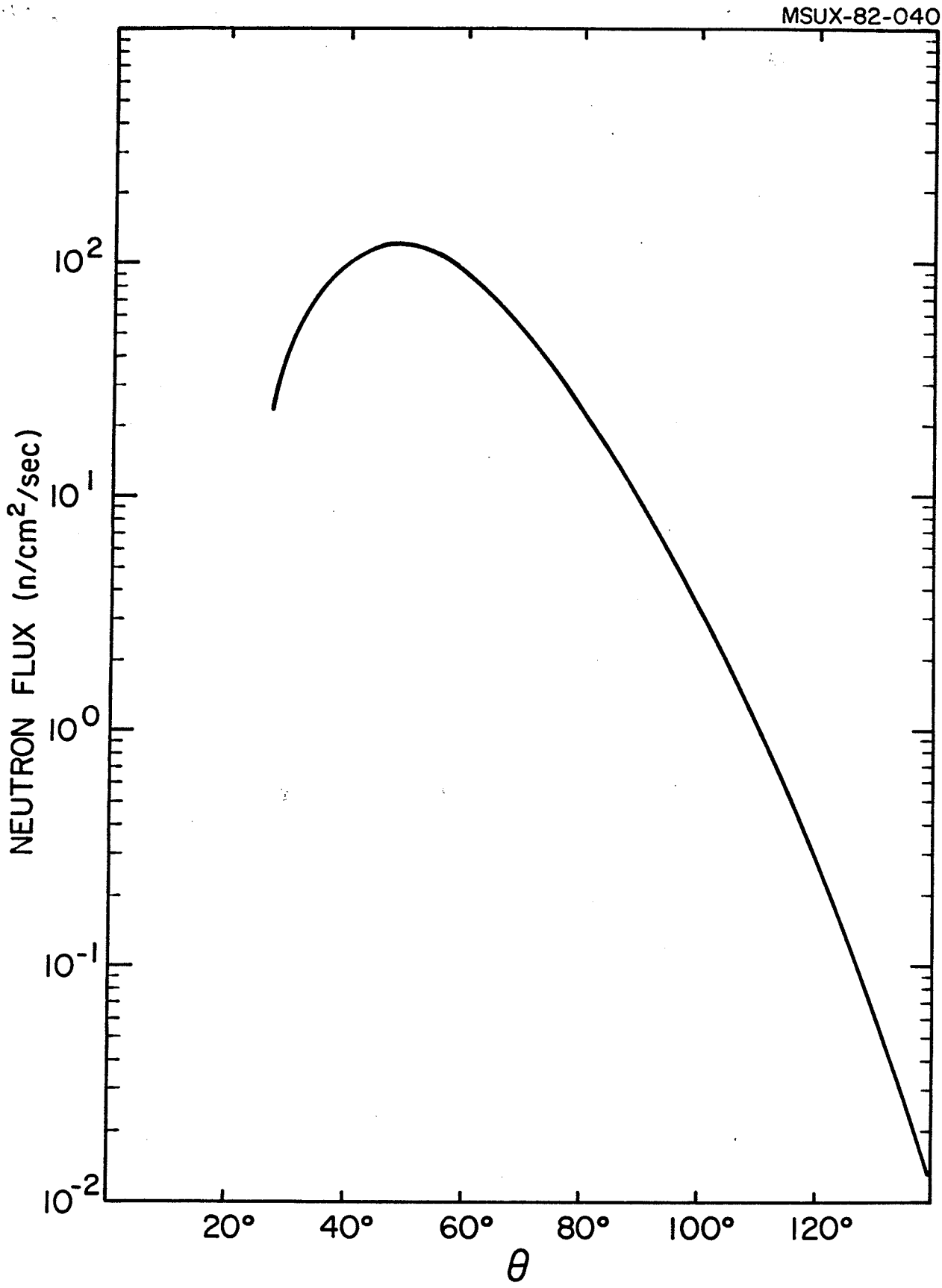
MSUX-82-040
NEUTRON FLUX (n/cm²/sec)
10²
10¹
10⁰
10⁻¹
10⁻²
20°
40°
60°
80°
100°
120°
θ

MSUX-82-037

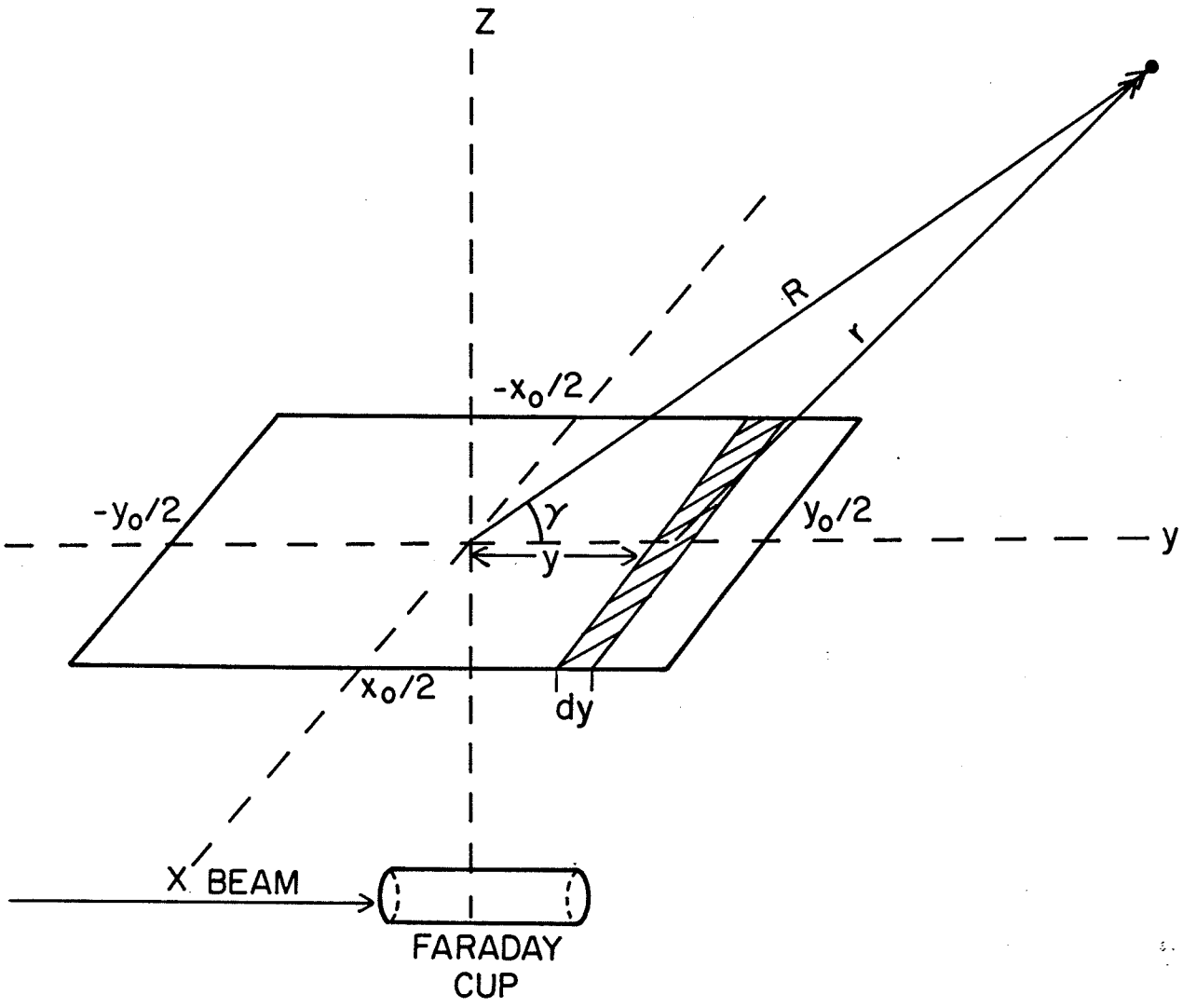

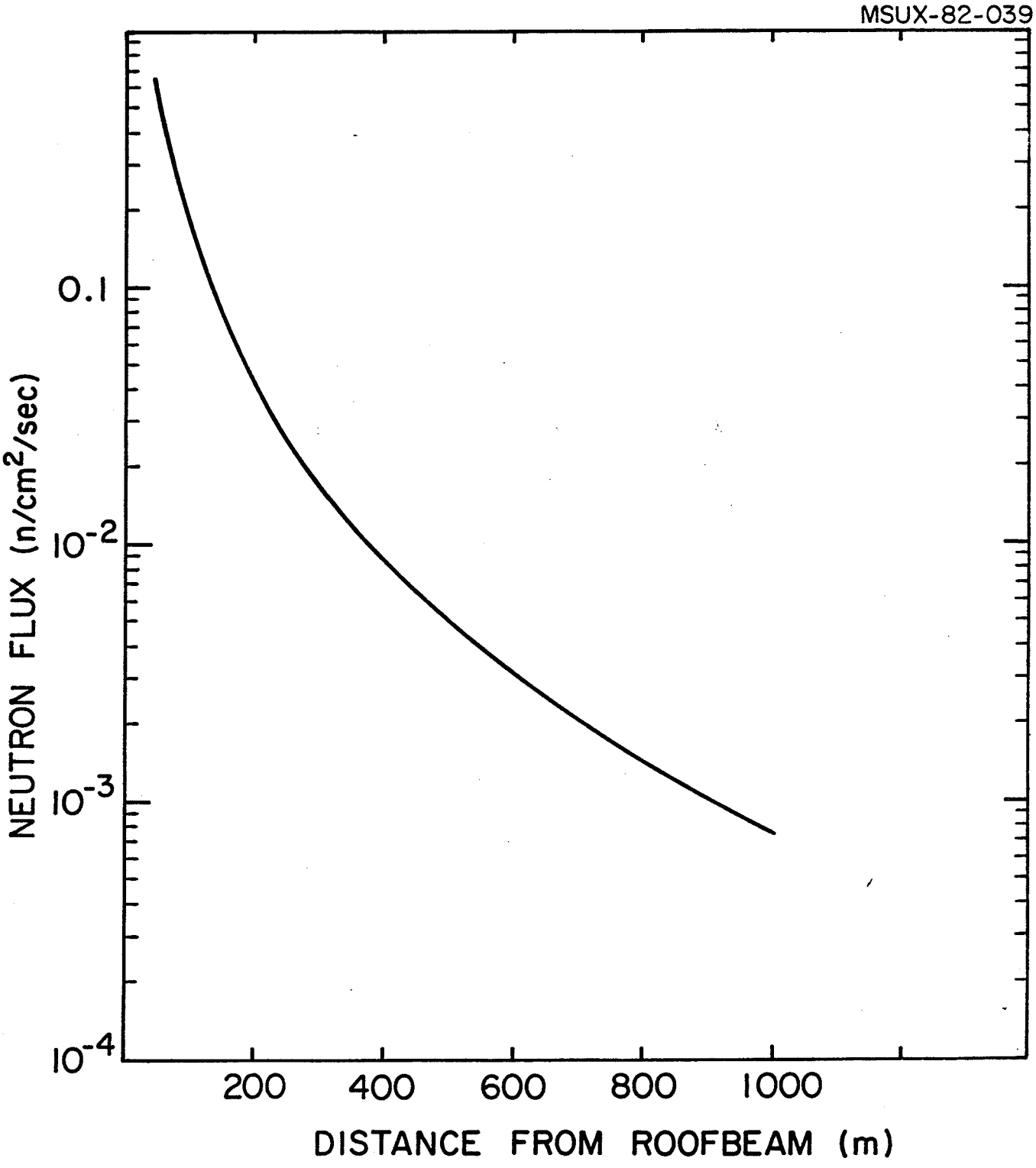
MSUX-82-039
0.1
10^{-2}
10^{-3}
10^{-4}
NEUTRON FLUX (n/cm^2/sec)
200
400
600
800
1000
DISTANCE FROM ROOFBEAM (m)